Consistent 3D Model Construction with Autonomous Mobile Robots

Andreas Nüchter, Hartmut Surmann, Kai Lingemann, and Joachim Hertzberg

Fraunhofer Institute for Autonomous Intelligent Systems (AIS)
Schloss Birlinghoven, D-53754 Sankt Augustin, Germany
{nuechter|surmann|lingemann|hertzberg}@ais.fraunhofer.de

Abstract. Digital 3D models of the environment are needed in facility management, architecture, rescue and inspection robotics. To create 3D volumetric models of scenes, rooms or buildings, it is necessary to gage several 3D scans and to merge them into one consistent 3D model. This paper presents a system, composed of a fast and robust, autonomous mobile robot, a precise, cost effective, high quality 3D laser scanner, and reliable scan matching algorithms for measuring and reconstructing environments, capable of matching two 3D scans within a fraction of a second.
The proposed new software modules for scan matching are fast variants of the iterative closest point algorithm (ICP) for consistent alignment. Two applications are presented: First, the reconstruction of an office environment, second, the fitting of sewer pipes into 3D data to detect deviations from the spatial geometry.

1 Introduction

3D digitalization of environments without occlusions requires multiple 3D scans. Autonomous mobile robots equipped with a 3D laser range finder are well suited for gaging the 3D data. Due to odometry errors, the self localization of the robot is an unprecise measurement and therefore cannot be relied on for registration of the 3D scans in a common coordinate system. The geometric structure of overlapping 3D scans has to be considered. Our approach uses a newly developed, fast version of the well known Iterative Closest Point (ICP) algorithm, a method for aligning three dimensional models purely based on the geometry.

To build complete volumetric models, multiple 3D scans have to be registered. Most published registration methods concentrate on pairwise alignment of two 3D scans. Pulli concludes that extending these pairwise methods for a multiview case has proven not to be straightforward, since simply chaining pairwise registration over all scans seldom works [13]. The goal of the work presented here is to develop a method that does work. To acquire the multiple 3D scans a robot equipped with the AIS 3D laser range finder explores the world and creates reliably a precise and consistent 3D volumetric representation, in real-time.

Instead of using 3D scanners, which yield consistent 3D scans in the first place, some groups have attempted to build 3D volumetric representations of

environments with 2D laser range finders. Thrun et al. [10, 21], Früh et al. [8] and Zhao et al. [23] use two 2D laser range finder for acquiring 3D data. One laser scanner is mounted horizontally, the other vertically. The latter one grabs a vertical scan line which is transformed into 3D points using the current robot pose. Since the vertical scanner is not able to scan sides of objects, Zhao et al. use two additional vertical mounted 2D scanner shifted by 45° to reduce occlusion [23]. The horizontal scanner is used to compute the robot pose. The precision of 3D data points depends on that pose and on the precision of the scanner.

A few other groups use 3D laser scanners [16, 1]. The RESOLV project aimed at modeling interiors for virtual reality and tele-presence [16]. They used a RIEGL laser range finder on robots and the ICP algorithm for scan matching [4, 6, 22]. The AVENUE project develops a robot for modeling urban environments [1], using a CYRAX laser scanner and a feature-based scan matching approach for registration of the 3D scans in a common coordinate system [18]. The research group of M. Hebert has reconstructed environments using the Zoller+Fröhlich laser scanner and aims to build 3D models without initial position estimates, i.e., without odometry information [11].

The paper is organized as follows. Sections 2 and 3 describe the used 3D laser range finder and the mobile robots. Section 4 presents the scan matching, followed by the application of matching sewer pipes in section 5. Section 6 concludes.

2 The AIS 3D Laser Range Finder

The AIS 3D laser range finder (Fig. 1) [19] is built on the basis of a 2D range finder by extension with a mount and a small servomotor. The 2D laser range finder is attached in the center of rotation to the mount for achieving a controlled pitch motion. A standard servo is connected on the left side (Fig. 1) and is controlled by the computer running RT-Linux, a real-time operating system which runs LINUX as a task with lowest priority [19, 20]. The 3D laser scanner operates up to 5h (Scanner: 17 W, 20 NiMH cells with a capacity of 4500 mAh, Servo: 0.85 W, 4.5 V with batteries of 4500 mAh) per battery pack.

The area of $180°(\text{h}) \times 120°(\text{v})$ is scanned with different horizontal (181, 361, 721) and vertical (128, 256) resolutions. A plane with 181 data points is scanned in 13 ms by the 2D laser range finder (rotating mirror device). Planes with more data points, e.g., 361, 721, duplicate or quadruplicate this time. Thus a scan with 181×256 data points needs 3.4 seconds. In addition to the distance measurement the 3D laser range finder is capable of quantifying the amount of light returning to the scanner. Fig. 2 (top row) shows an example of a reflectance image of the GMD-Robobench, a standard office environment for the evaluation of autonomous robots. The left image gives an distorted view of the scene: One scan line of the figure corresponds to a slice of the 2D scanner, the rotation of the scanner is not considered. The right image shows the scene with the distortions corrected.

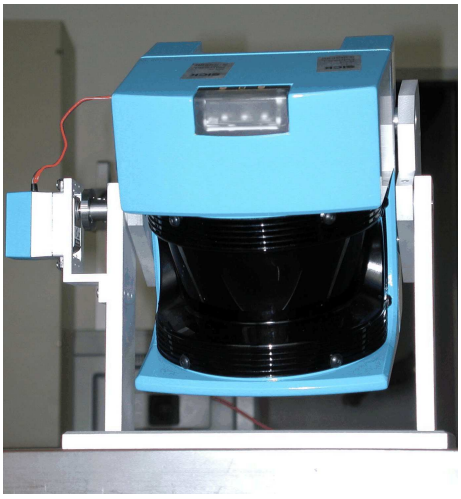

Fig. 1. The AIS 3D laser range finder. Its technical basis is a SICK 2D laser range finder (LMS-200).

The basis of the scan matching are algorithms for reducing points and detecting lines. Next we give a brief description of these algorithms. Details can be found in [19, 20].

The scanner emits the laser beams in a spherical way, such that the data points close to the source are more dense. The first step is to reduce the data. Therefore, data points located close together are joined into one point. The number of these *reduced points* is one order of magnitude smaller than before (Fig. 6 (right)). Furthermore noise within the data is reduced [20].

Second a simple length comparison is used as a line detection algorithm. Given that the anticlockwise ordered data of the laser range finder (points $a_0, a_1, \ldots, a_n$) are located on a line, then for a_{j+1} the algorithm has to check if $\|a_i, a_{j+1}\| \ / \ \sum_{t=i}^{j} \|a_t, a_{t+1}\| < \epsilon(j)$ to determine if a_{j+1} is on line with a_j.

3 The Autonomous Mobile Robots

The Ariadne Robot (Fig. 3, left) is based on a commercial DTV and is about 80 cm × 60 cm large and 90 cm high. The mobile platform can carry a payload of 200 kg at speeds of up to 0.8 m/s (about half the speed of a pedestrian). The right and left driving wheels are mounted on a suspension on the center line of the mobile platform. Passive castors on each corner of the chassis ensure stability. The core of the robot is a Pentium-III-800 MHz with 384 MB RAM and real-time Linux. One embedded PC-104 system is used to control the motor, internal display and numerical keyboard and radio link of the robot. The platform is rigged with two 2D safety laser scanners as bumper substitutes, one on the front

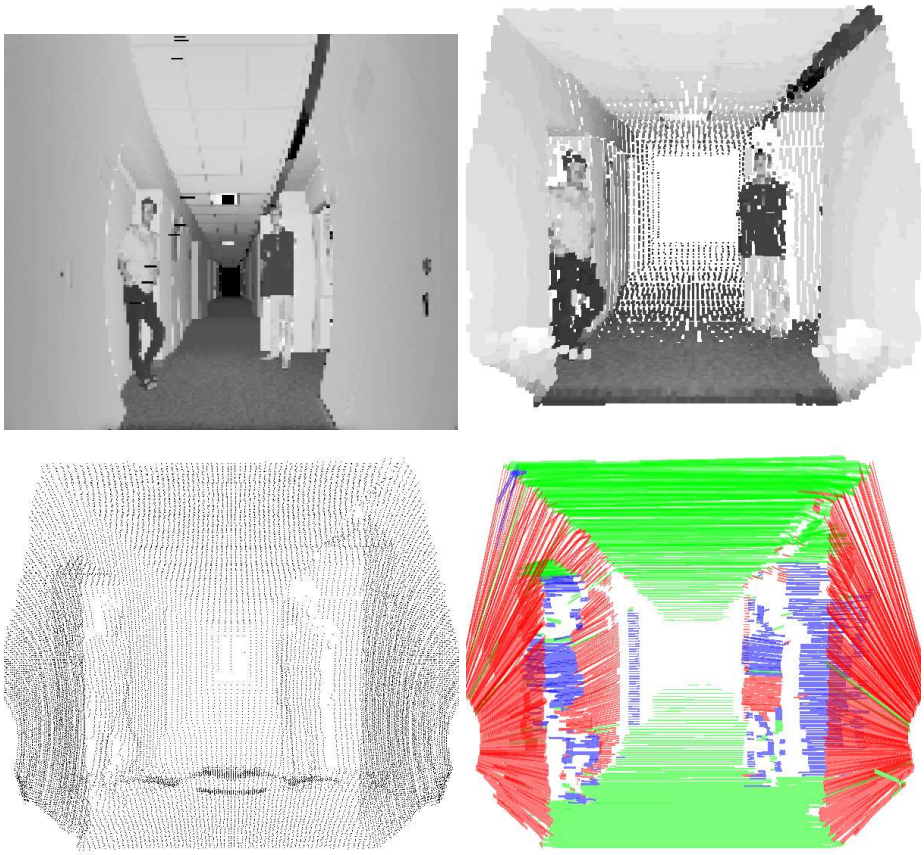

Fig. 2. Two persons standing in a corridor of an office building (GMD Robobench). Top left: Reflectance image (distorted). Top right: Corrected reflectance image with distant points clipped. Bottom left: All points. Bottom right: Result of line detection with orientation.

and the other on the rear of the robot. Each laser scans a horizontal plane of 180° of the environment. The robot has a weight of 250 kg and operates for about 8 hours with one battery charge.

KURT2 (Fig. 3, left) is a mobile robot platform with a size of 45 cm (length) × 33 cm (width) × 26 cm (hight) and a weight of 15.6 kg. Equipped with the 3D laser range finder the height increases to 47 cm and weight increases to 22.6 kg. KURT2's maximum velocity is 5.2 m/s (autonomously controlled 4.0 m/s). Two 90W motors are used to power the 6 wheels, whereas the front and rear wheels have no tread pattern to enhance rotating. KURT2 operates for about

Fig. 3. Left: The Ariadne robot platform. Right: KURT2. Both systems can be equipped with the the AIS 3D laser range finder.

4 hours with one battery (28 NiMH cells, capacity: 4500 mAh) charge. The core of the robot is a Pentium-III-600 MHz with 384 MB RAM and real-time Linux. An embedded 16-Bit CMOS microcontroller is used to control the motor.

4 Range Image Registration

Multiple 3D scans are necessary to digitalize environments without occlusions. To create a correct and consistent model, the scans have to be merged into one coordinate system. This process is called registration. If the localization of the robot with the 3D scanner were precise, the registration could be done directly by the robot pose. However, due to the unprecise robot sensors, the self localization is erroneous, so the geometric structure of overlapping 3D scans has to be considered for registration.

Scan matching approaches can be classified into two categories:

Matching as an optimization problem uses a cost function for the quality of the alignment of the scans. The range images are registered by determining the rigid transformation (rotation and translation) which minimizes the cost function.

Feature based matching extracts distinguishing features of the range images and uses corresponding features for calculating the alignment of the scans.

The matching of 3D scans can either operate on the whole three-dimensional scan point set or can be reduced to the problem of scan matching in 2D by extracting, e.g., a horizontal plane of fixed height from both scans, merging these 2D scans and applying the resulting translation and rotation matrix to all points of the corresponding 3D scan.

Matching of complete 3D scans has the advantage of having a larger set of attributes (either pure data points or extracted features) to compare the scans. This results in higher precision and lowers the possibility of running into a local minimum of the cost function. Furthermore, using three dimensions enables the robot control software to recognize and take into account changes of height and roll, yaw and pitch angles of the robot. This is essential for robots driving cross country and in pipes.

4.1 Matching as an Optimization Problem

The following method for registration of point sets is part of many publications, so only a short summary is given here. The complete algorithm was invented in 1991 and can be found, e.g., in [4, 6, 22]. The method is called *Iterative Closest Points (ICP) algorithm*.

Given two independently acquired sets of 3D points, M (model set, $|M| = N_m$) and D (data set, $|D| = N_d$) which correspond to a single shape, we want to find the transformation consisting of a rotation $\mathbf{R}$ and a translation $\mathbf{t}$ which minimizes the following cost function:

$$E(\mathbf{R}, \mathbf{t}) = \sum_{i=1}^{N_m} \sum_{j=1}^{N_d} w_{i,j} \left|\left|\mathbf{m}_i - (\mathbf{R}\mathbf{d}_j + \mathbf{t})\right|\right|^2 . \tag{1}$$

$w_{i,j}$ is assigned 1 if the i-th point of M describes the same point in space as the j-th point of D. Otherwise $w_{i,j}$ is 0. Two things have to be calculated: First, the corresponding points, and second, the transformation ($\mathbf{R}$, $\mathbf{t}$) that minimize $E(\mathbf{R}, \mathbf{t})$ on the base of the corresponding points.

The ICP algorithm calculates iteratively the point correspondences. In each iteration step, the algorithm selects the closest points as correspondences and calculates the transformation $(\mathbf{R}, \mathbf{t})$ for minimizing equation (1). Besl et al. proves that the method terminates in a minimum [4]. The assumption is that in the last iteration step the point correspondences are correct.

In each iteration, the transformation is calculated by the quaternion-based method of Horn [12]. A unit quaternion is a 4 vector $\dot{q} = (q_0, q_x, q_y, q_z)^T$, where $q_0 \geq 0, q_0^2 + q_x^2 + q_y^2 + q_z^2 = 1$. It describes a rotation axis and an angle to rotate around that axis. A 3×3 rotation matrix $\mathbf{R}$ is calculated from the unit quaternion according the the following scheme:

$$\mathbf{R} = \begin{pmatrix} (q_0^2 + q_x^2 - q_y^2 - q_z^2) & 2(q_x q_y + q_z q_0) & 2(q_x q_z + q_y q_0) \\ 2(q_x q_y + q_z q_0) & (q_0^2 - q_x^2 + q_y^2 - q_z^2) & 2(q_y q_z - q_x q_0) \\ 2(q_z q_x - q_y q_0) & 2(q_z q_y + q_x q_0) & (q_0^2 - q_x^2 - q_y^2 + q_z^2) \end{pmatrix} .$$

To determine the transformation, the mean values (centroid vectors) $\mathbf{c}_m$ and $\mathbf{c}_d$ are subtracted from all points in M and D, respectively, resulting in the sets M' and D'. The rotation expressed as quaternion that minimizes equation (1)

is the largest eigenvalue of the cross-covariance matrix

$$\mathbf{N} = \begin{pmatrix} (S_{xx}+S_{yy}+S_{zz}) & (S_{yz}+S_{zy}) & (S_{zx}+S_{xz}) & (S_{xy}+S_{yx}) \\ (S_{yz}+S_{zy}) & (S_{xx}-S_{yy}-S_{zz}) & (S_{xy}+S_{yx}) & (S_{zx}+S_{xz}) \\ (S_{zx}+S_{xz}) & (S_{xy}+S_{yx}) & (-S_{xx}+S_{yy}-S_{zz}) & (S_{yz}+S_{zy}) \\ (S_{xy}+S_{yx}) & (S_{yz}+S_{zy}) & (S_{zx}+S_{xz}) & (-S_{xx}-S_{yy}+S_{zz}) \end{pmatrix},$$

with $S_{\alpha\beta} := \sum_{i=1}^{N_m} \sum_{j=1}^{N_d} w_{i,j} m'_{i\alpha} d'_{j\beta}$. After the calculation of the rotation $\mathbf{R}$, the translation is $\mathbf{t} = \mathbf{c}_m - \mathbf{R}\mathbf{c}_d$ [12]. Fig. 4 shows three steps of the ICP algorithm in registering two 3D scans in our GMD Robobench environment[1].

The time complexity of the algorithm mainly depends on determination of the closest points (brute force search $O(n^2)$ for 3D scans of n points). Several enhancements have been proposed [4, 17]. We have implemented kd-trees as proposed by Simon et al., combined with the above-described *reduced points*. Table 1 summarizes the results of different experiments on a Pentium-III-800. The starting point for optimization is given by the robot odometry.

Table 1. Computing time of the different 3D scan matching implementations for two scans of the GMD Robobench (Fig. 4). The number of all points is 46336 (181 × 256) and the number of the *reduced points* is 4910.

points used	time	# iter.
all points & brute force	3 hours 47 min	27
reduced points & brute force	3 min 6 sec	25
all points & kD–tree	6 sec	27
reduced points & kD–tree	<1.4 sec	25

4.2 Matching Multiple 3D Scans

To digitalize environments without occlusions, multiple 3D scans have to be registered. After registration, the scene has to be globally consistent. A straightforward method for aligning several 3D scans is *pairwise matching*, i.e., the new scan is registered against the scan with the largest overlapping areas. The latter one is determined in a preprocessing step. Alternatively, Chen and Medioni [6] introduced an *incremental matching* method, i.e., the new scan is registered against a so-called *metascan*, which is the union of the previously acquired and registered scans. Each scan matching has a limited precision. Both methods accumulate the registration errors such that the registration of many scans leads to inconsistent scenes (Fig. 5) and to problems with the robot localization.

Pulli presents a registration method that minimizes the global error and avoids inconsistent scenes [13]. This method distributes the global error while the registration of one scan is followed by registration of all neighboring scans.

[1] For an animation of this result please refer to the following website: `http://www.ais.fhg.de/ARC/3D/videos`.

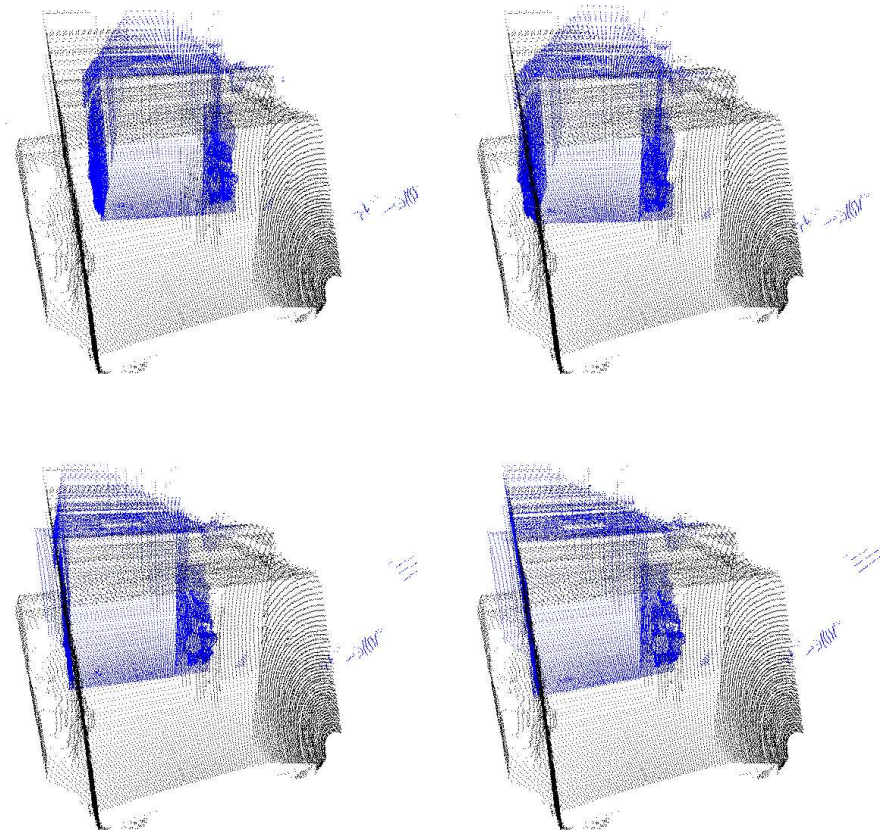

Fig. 4. Registration of two 3D-scans of an office environment with the ICP algorithm. Top left: Initial alignment based on odometry. Top right: Alignment after 2 iterations. Bottom left: after 5 iterations. Bottom right: Final alignment after 25 iterations. The scans correspond to Fig. 2. The number of sampled 3D points is 46336 per 3D scan and the number of *reduced points* is 4910.

Other matching approaches with global error minimization have been published, e.g., by Benjemaa et. al. [2] and Eggert et. al. [7].

Based on the idea of Pulli we have designed a method called *simultaneous matching*. Here, the first scan is the masterscan and determines the coordinate system. This scan is fixed. The following steps register all scans and minimize the global error:

1. Based on the robot odometry, pairwise matching is used to find a start registration for each new scan. This step speeds up computation.

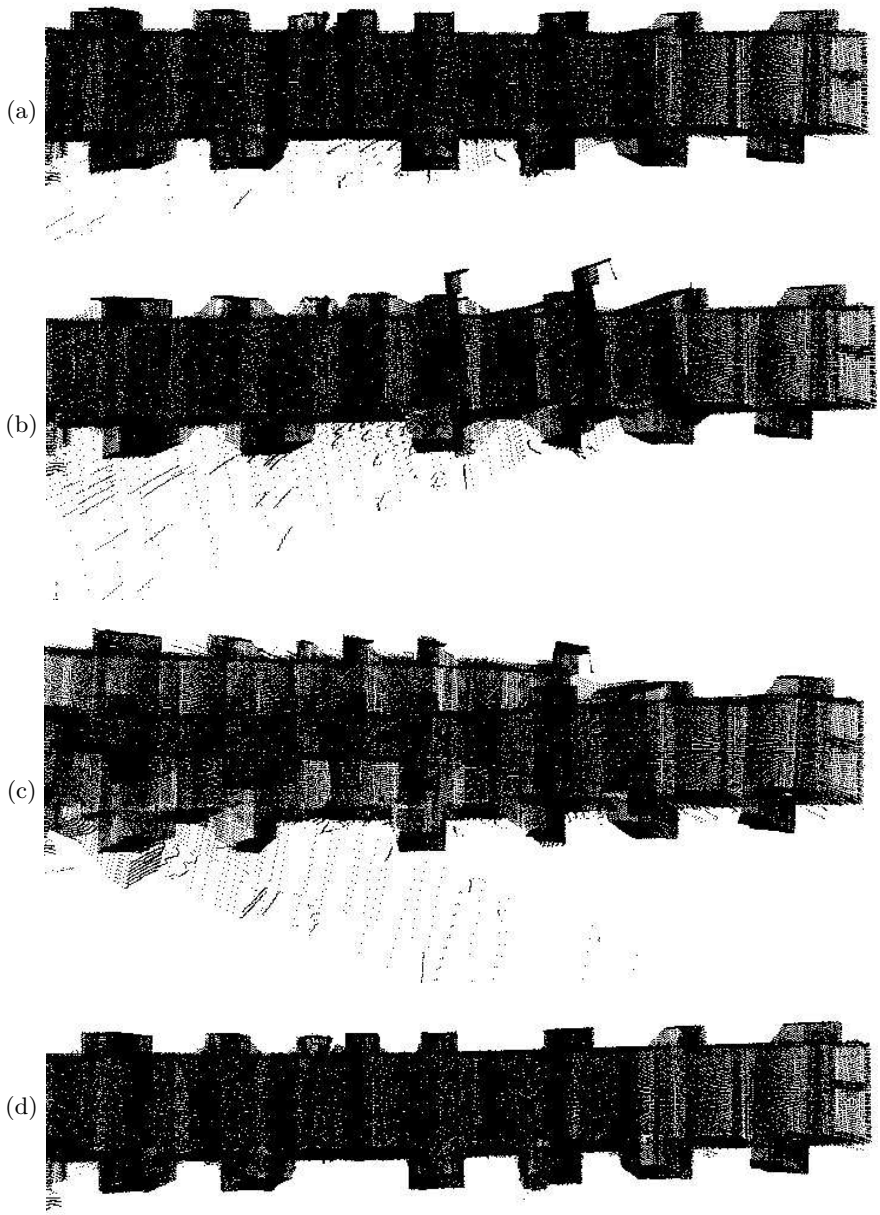

Fig. 5. Results of the scan matching of 20 scans (top view). All 3D scans were taken in an office environment, the GMD Robobench, the first one corresponds to Fig. 2. (a) Pairwise matching, (b) incremental matching, (c) 3D scan matching with edge points and (d) simultaneous matching. 3D animations can be found at `http://www.ais.fhg.de/ARC/3D/videos`.

2. A queue is initialized with the new scan.
3. Three steps are repeated until the queue is empty:
   (a) The current scan is the first scan of the queue. This scan is removed from the queue.
   (b) If the current scan is not the master scan, then a set of neighbors (set of all scans that overlap with the current scan) is calculated. This set of neighbors form one point set M. The current scan forms the data point set D and is aligned with the ICP algorithm.
   (c) If the current scan changes its location by applying the transformation, then each single scan of the set of neighbors that is not in the queue, is added to the end of the queue.

Note: One scan overlaps with another, iff more than 250 corresponding point pairs exist. To speed up the matching, kD trees and *reduced points* are used (see Table 1).

In contrast to Pulli's approach, the proposed method is totally automatic and no interactive pairwise alignment needs to be done. Furthermore the point pairs are not fixed [13]. Fig. 5 shows results of the scan matching using 20 scans taken in the GMD Robobench. Pairwise matching (a) works sufficient, incremental matching shows most outliers (b), and simultaneous matching (d) reconstructs the corridor perfectly.

4.3 Feature Based Matching

Sappa et al. suggest to extract edge points and use them for the creating point pairs [15]. Based on our line representation of the scene (Fig. 2, bottom right) the end points of every line are used to create an edge base representation. Fig. 6 (left) shows an edge-based representation in comparison with the *reduced points* (right). Fig. 5 (c) shows the result of the registration process with the edge points (pairwise matching). The registration speed is good due to the lower number of points. Unfortunately, the matching results are insufficient for office environments, because of the simple structure of the scanned scene. The office environment (corridors) mainly consists of floor, ceiling and walls.

4.4 Scanning in dynamic environments

Dynamic objects lead to errors in the resulting 3D volumetric model with artefacts or misalignments. Misalignments result in an incorrect self localization of the mobile robot. To eliminate these errors, the robot monitors the environment with its other sensors, e.g., the horizonal mounted 2D laser range finders or cameras. If the sensors detect dynamic objects with the method of the differential frames, the robot simply repeats the 3D scan. Data points belonging to dynamic objects are not yet isolated and removed.

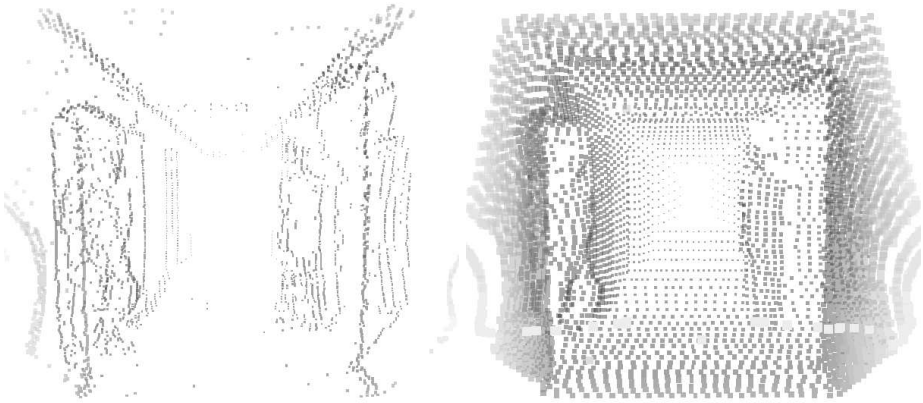

Fig. 6. Left: The scanned scene of the GMD Robobench (see Fig. 2) in an edge based representation using the simple line detection routine. Right: 4910 *reduced points* (enlarged).

5 Mapping Shapes with Scan Matching

Another application of the ICP algorithm is the mapping of arbitrary shapes into a scanned scene. For a given shape, the model set M is computed by calculating the closest points from an abstract description of the shape, e.g., a plane for mapping a wall, or a cuboid for mapping an office cubicle. Similar to minimizing the total error between two sets of points, the selected shape is being transformed (rotated & translated) in order to match it into the given scene.

5.1 Matching Sewerage Pipes

Inspecting communal sewer systems is a potential application for mobile robots [3, 14]. Two basic problems of such inspection robots are self localization and the reconstruction of the sewerage pipe system. These problems are addressed in this section. Similar to matching sewerage pipes is the problem of mapping cylinders in 3D data, which is well known in the reconstruction of industrial environments with pipes and tubes [5]. State of the art is semi-automatic reconstruction [9].

For matching tubes into scanned pipes, the closest point on the pipe surface is calculated as follows: Given a scan point $\mathbf{x} \in \mathbb{R}^3$ and a pipe, described by two points $\mathbf{a}$ and $\mathbf{b}$ ($\mathbf{a}, \mathbf{b} \in \mathbb{R}^3$) and the radius r (Fig. 7), the closest point $\mathbf{c}$ to $\mathbf{x}$ on the pipe surface is

$$\mathbf{n} = \frac{\mathbf{a} - \mathbf{b}}{\|\mathbf{a} - \mathbf{b}\|} , \qquad s = \frac{< \mathbf{x} - \mathbf{a}, \mathbf{n} >}{< \mathbf{n}, \mathbf{n} >} \tag{2}$$

$$\mathbf{c} = s \cdot \mathbf{n} + r \cdot \frac{\mathbf{x} - s \cdot \mathbf{n}}{\|\mathbf{x} - s \cdot \mathbf{n}\|} \tag{3}$$

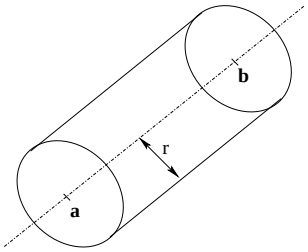

Fig. 7. A sewerage pipe is modeled by two points **a** and **b** and the radius r.

with **n** the norm vector between **a** and **b** and s the projection of **x** to **n**.

The following steps match pipes with the pipe model:

1. A default tube is inserted into the 3D scan to initialize the matching (Fig. 8 top left).
2. An optimal rotation and translation matrix is calculated with the ICP algorithm (Fig. 8 top right).
3. The radius of the tube is gradually enlarged or reduced until the tube matches the 3D points, i.e., until the error function of the ICP algorithm is minimal (Fig. 8 bottom).

At the beginning, the last two steps are iterated with a reduced number of points to rapidly calculate the transformations. Finally the matching is refined with all points. The result is given in Fig. 8 and 9.[2]

With the proposed matching, a pipe is reconstructed. Due to the exact matching of the tube and the high precision of the scanner, deviations and abnormalities like pipe deformations are also detected. Furthermore obstacles, e.g., a brick as given in the middle picture of Fig. 9 are found. The self localization of the robot is improved, because the transformations calculated by the matching process is applied inversely to the robot pose.

6 Conclusions

3D digitalization of environments without occlusions requires multiple 3D scans. This paper has presented a system, composed of an autonomous mobile robot, a 3D laser scanner, and scan matching algorithms for measuring and reconstructing of environments. Basic scan matching algorithms based on the ICP algorithm have been accelerated and extended to consistent multiview scan registration. A sophisticated reduction of scan points enables to maintain soft real time constraints in 3D scan matching. Multiview registration (simultaneous matching) based on the mutually alignment of a 3D scan with its neighbors generate overall consistent scenes.

[2] For an animation of the matching process please visit:
`http://www.ais.fhg.de/ARC/3D/tube.gif`.

Fig. 8. Matching of a tube into a scanned sewerage pipe (first the tube is being rotated & translated into the correct position, then the size is being adapted)

Several applications, namely, the 3D reconstruction and modeling, deviation and deformation detection and 3D obstacle detection, have been presented. The algorithms have been tested in two different environments, i.e., in indoor, office environments and sewerage pipes. Further applications, e.g., deformation detection in sewer pipes have to be tested. An additional advantage of the proposed systems is that the AIS 3D laser range finder measures actively distances and reflections. Vision-based approaches for sewerage pipes need additional power consuming light sources.

Future work will concentrate on more experiments in sewerage pipes, on scene interpretation, view point planning and on sensor fusion with camera images for office environments.

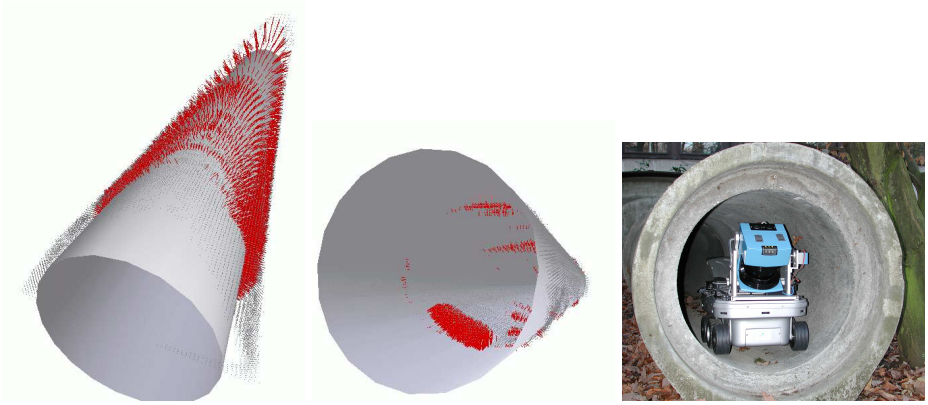

Fig. 9. Distances between scanned points and ideal tube. Left: A tube with point-to-tube vectors and *without* adjusted radius. Middle: Fully processed tube with an obstacle (a brick). Right: KURT2 inside of a test sewer network.

References

1. P. Allen, I. Stamos, A. Gueorguiev, E. Gold, and P. Blaer. AVENUE: Automated Site Modelling in Urban Environments. In *Proceedings of the Third International Conference on 3D Digital Imaging and Modeling (3DIM '01)*, Quebec City, Canada, May 2001.
2. R. Benjemaa and F. Schmitt. Fast Global Registration of 3D Sampled Surfaces Using a Multi-Z-Buffer Technique. In *Proceedings IEEE International Conference on Recent Advances in 3D Digital Imaging and Modeling (3DIM '97)*, Ottawa, Canada, May 1997.
3. K. Berns, Th. Christaller, R. Dillmann, J. Hertzberg, W. Ilg, M. Kemmann, E. Rome, and H. Stapelfeldt. LAOKOON – lernfähige autonome kooperierende Kanalroboter. *KI*, 11(2):28 – 32, 1997.
4. P. Besl and N. McKay. A method for Registration of 3–D Shapes. *IEEE Transactions on Pattern Analysis and Machine Intelligence*, 14(2):239 – 256, February 1992.
5. Th. Chaperon and F. Goulette. Extracting Cylinders in Full 3-D Data Using a Random Sampling Method and the Gaussian Image. In *Proceedings of the of the 6th International Fall Workshop Vision, Modeling, and Visualization (VMV '01)*, Stuttgart, Germany, November 2001.
6. Y. Chen and G. Medoni. Object Modelling by Registration of Multiple Range Images. In *Proceedings of the IEEE Conferenc on Robotics and Automation (ICRA '91)*, pages 2724 – 2729, Sacramento, CA, USA, April 1991.
7. D. Eggert, A. Fitzgibbon, and R. Fisher. Simultaneous Registration of Multiple Range Views Satisfying Global Consistency Constraints for Use In Reverse Engineering. *Computer Vision and Image Understanding*, 69:253 – 272, March 1998.
8. C. Früh and A. Zakhor. 3D Model Generation for Cities Using Aerial Photographs and Ground Level Laser Scans. In *Proceedings of the Computer Vision and Pattern Recognition Conference (CVPR '01)*, Kauai, Hawaii, USA, December 2001.

9. F. Haertl and Chr. Fröhlich. Semi-Automatic 3D CAD Model Generation of As-Built Conditions of Real Environmentsusing a Visual Laser Radar. In *Proceedings of the 10th IEEE International Workshop on Robot-Human Interactive Communication (ROMAN '01)*, Paris, France, September 2001.
10. D. Hähnel, W. Burgard, and S. Thrun. Learning Compact 3D Models of Indoor and Outdoor Environments with a Mobile Robot. In *Proceedings of the fourth European workshop on advanced mobile robots (EUROBOT '01)*, Lund, Sweden, September 2001.
11. M. Hebert, M. Deans, D. Huber, B. Nabbe, and N. Vandapel. Progress in 3–D Mapping and Localization. In *Proceedings of the 9th International Symposium on Intelligent Robotic Systems, (SIRS '01)*, Toulouse, France, July 2001.
12. B. Horn. Closed–form solution of absolute orientation using unit quaternions. *Journal of the Optical Society of America A*, 4(4):629 – 642, April 1987.
13. K. Pulli. Multiview Registration for Large Data Sets. In *Proceedings of the 2nd International Conference on 3D Digital Imaging and Modeling (3DIM '99)*, pages 160 – 168, Ottawa, Canada, October 1999.
14. E. Rome, J. Hertzberg, Th. Christaller, F. Kirchner, and U. Licht. Towards Autonomous Sewer Robots: The MAKRO Project. *Journal Urban Water*, 1:57 – 70, 1999.
15. A. Sappa, A. Restrepo-Specht, and M. Devy. Range Image Registration by using an Edge–based Representation. In *Proceedings of th 9th International Symposium on Intelligent Robotic Systems, (SIRS '01)*, Toulouse, France, July 2001.
16. V. Sequeira, K. Ng, E. Wolfart, J. Goncalves, and D. Hogg. Automated 3D reconstruction of interiors with multiple scan–views. In *Proceedings of SPIE, Electronic Imaging '99, The Society for Imaging Science and Technology /SPIE's 11th Annual Symposium*, San Jose, CA, USA, January 1999.
17. D. Simon, M. Hebert, and T. Kanade. Real–time 3–D pose estimation using a high–speed range sensor. In *Proceedings of IEEE International Conference on Robotics and Automation (ICRA '94)*, volume 3, pages 2235 – 2241, San Diego, CA, USA, May 1994.
18. I. Stamos and P. Allen. 3-D Model Construction Using Range and Image Data. In *Proceedings of the Conference on Computer Vision and Pattern Recognition (CVPR '00)*, USA, June 2000.
19. H. Surmann, K. Lingemann, A. Nüchter, and J. Hertzberg. A 3D laser range finder for autonomous mobile robots. In *Proceedings of the of the 32nd International Symposium on Robotics (ISR '01)*, pages 153 – 158, Seoul, Korea, April 2001.
20. H. Surmann, K. Lingemann, A. Nüchter, and J. Hertzberg. Fast acquiring and analysis of three dimensional laser range data. In *Proceedings of the of the 6th International Fall Workshop Vision, Modeling, and Visualization (VMV '01)*, pages 59 – 66, Stuttgart, Germany, November 2001.
21. S. Thrun, D. Fox, and W. Burgard. A real-time algorithm for mobile robot mapping with application to multi robot and 3D mapping. In *Proceedings of the IEEE International Conference on Robotics and Automation (ICRA '00)*, San Francisco, CA, USA, April 2000.
22. Z. Zhang. Iterative point matching for registration of free–form curves. Technical Report RR-1658, INRIA–Sophia Antipolis, Valbonne Cedex, France, 1992.
23. H. Zhao and R. Shibasaki. Reconstructing Textured CAD Model of Urban Environment Using Vehicle-Borne Laser Range Scanners and Line Cameras. In *Second International Workshop on Computer Vision System (ICVS '01)*, pages 284 – 295, Vancouver, Canada, July 2001.